



REMIBRANDT: Imputing Radio Environmental Maps for Safety-Critical Applications with Machine Learning

Nils Altenburg, Hendrik Schippers, Melina Geis, and Christian Wietfeld

Communication Networks Institute, TU Dortmund University, 44227 Dortmund, Germany
e-mail: {Nils.Altenburg, Hendrik.Schippers, Melina.Geis, Christian.Wietfeld}@tu-dortmund.de

Abstract—5G and future networks will enable new applications such as teleoperated driving, which demand proactive and error-free communication for mission-critical applications. Therefore, it is crucial to plan the vehicles' route in accordance with the available channel quality, which can be obtained, for instance, by utilizing Radio Environmental Maps (REMs). These can be generated by automated measurements. However, some areas of the Radio Environmental Map (REM) will inevitably still be sparse. In this work, we present a novel hybrid Machine Learning (ML)-driven approach, named REMIBRANDT, to impute missing signal strength information by incorporating surrounding geospatial data and neighboring measurements. The data is considered in an angularly distributed pattern, which enhances the ability of the employed Random Forest (RF) model to learn spatial structures. This approach does not require base station information, unlike previous methods, e.g., classic radio propagation models. REMIBRANDT outperforms the RMSE of the best-performing analytical model by 3 dB. Furthermore, compared to state-of-the-art solutions, the prediction of suitable Operational Design Domains (ODDs) for teleoperation can be markedly enhanced using REMIBRANDT. This enables more anticipatory and, consequently, safer application planning in current and future mobile networks.

I. INTRODUCTION

Compared to preceding communication standards, 5G is designed to serve a broader range of applications across diverse vertical domains, including innovative smart city applications [1]. These solutions encompass Intelligent Transportation Systems (ITSs) and Connected Autonomous Vehicles (CAVs), which are dependent on a reliable mobile network connection in order to ensure functional safety and service availability [2]. In this context, teleoperation becomes particularly relevant as it offers operational flexibility to resolve situations where autonomous systems encounter difficulties. In such cases, human operators are able to assume control and safely navigate the vehicle. However, teleoperation is heavily dependent on Ultra Reliable Low Latency Communications (URLLC) to guarantee safety and responsiveness. That is especially challenging in areas with fluctuating network conditions or in environments with high network utilization. Consequently, it is essential to avoid these areas when planning vehicle routes. To this end, comprehensive network Key Performance Indicators (KPIs) must be provided, for instance as REMs [3]. However, it is not feasible to achieve full measurement coverage. The resulting areas of unknown channel quality should be appropriately

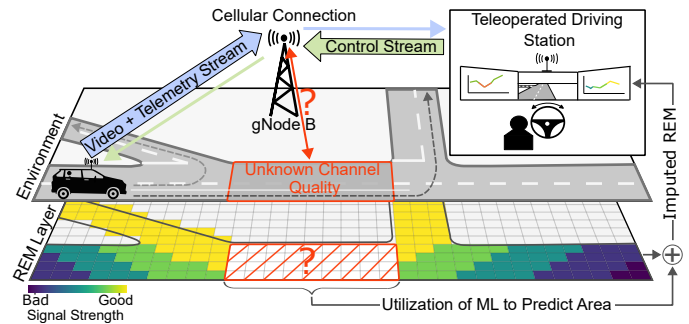


Fig. 1. A teleoperated vehicle facing an area with unknown channel quality may encounter difficulties. These can be solved by imputing the reference REM (Radio Environmental Map) and acting proactively.

filled, for instance by the imputation of existing neighboring KPIs.

Fig. 1 depicts an example scenario where a self-driving car must determine the optimal route to maintain sufficient channel quality for teleoperation to navigate challenging situations. Ideally, the decision is based on previously generated measurements, which may contain areas of unknown channel quality that require imputation to decide if channel conditions are sufficient to transmit the requisite streams.

In this paper, we present Radio Environmental Map Imputation using Machine Learning on Blank AREAs in Noisy DaTa (REMIBRANDT) as a novel approach for the imputation of missing data in Reference Signal Received Power (RSRP) REMs by incorporating surrounding geospatial data and neighboring RSRP values. REMIBRANDT relies on lightweight Machine Learning (ML) methods to achieve this. Previously captured comprehensive mobile network data of Dortmund, Germany, serves as the data basis [3]. This data was collected with the help of an automated measurement application in vast parts of the inner city and includes signal strength measurements for both 4G and 5G mobile networks.

The remainder of the paper is structured as follows. After discussing the related work in Sec. II, the proposed ML-based REM imputation method is described in Sec. III. Afterwards, an overview of the methodological aspects is given in Sec. IV. Finally, detailed results on the model accuracy and imputation performance in real-world scenarios are provided in Sec. V.

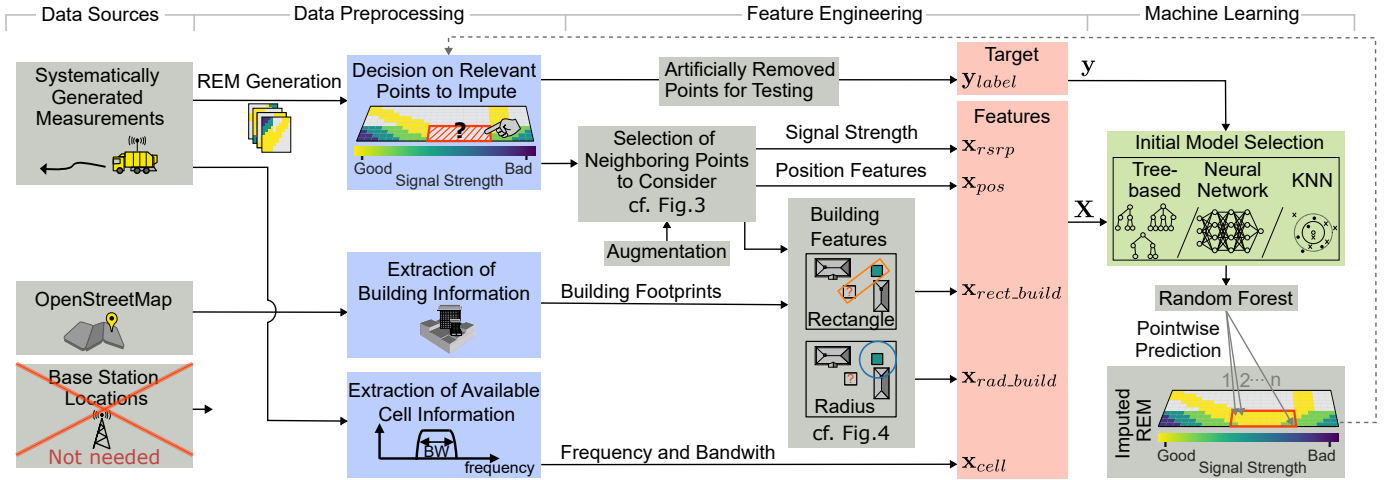


Fig. 2. Architecture of the proposed ML-based REMIBRANDT approach for imputation of REMs with missing areas.

II. RELATED WORK

As ML-enabled imputation of channel measurements is a rather new topic, it is limited in literature. However, missing areas in REMs can also be filled using other methods, e.g. classic or innovative ML-driven radio propagation models. In contrast to Imputation, which considers neighboring values, the path loss is determined solely based on a receiver and transmitter pair. Analytical models, such as Friis free space propagation or the two-ray ground model, can be used for this purpose. However, they are inaccurate due to the idealized assumptions about the environment. In contrast, empirical models, such as WINNER II [10] and Okumura Hata [11] rely on such comprehensive real-world measurements studies and scenario-specific model definitions. Many empirical models are based on the alpha-beta-gamma (ABG) model structure [12], which can also be utilized to fit the model parameters to custom measurement data. In contrast, ray tracing simulates the behavior of individual rays, requiring a comprehensive environment model. The quality of this model affects prediction accuracy; however, the computational cost is high.

In recent years, ML-based methods have become increasingly popular in channel quality prediction [13], as they

tend to be more accurate than empirical models and less computationally complex than ray-tracing models.

In [8] a Random Forest (RF) predicting the RSRP given a transmitter-receiver pair based on an extensive feature vector including also features derived from a 3D model of the environment is presented. A similar approach is followed by the authors in [9], where synthetic images derived from a 3D model of the environment are processed by a Convolutional Neural Network (CNN). In contrast, the authors in [6] introduce a model, where implicit environmental information are extracted by identifying empty regions in a K-Nearest Neighbor (KNN)-densified measurement REM. On that basis, a Deep Neural Network (DNN) is trained to predict the RSRP. However, like classic radio propagation models, the latter ML approaches require information on the Base Station (BS) position, which are typically not publicly available. [7] uses a Gaussian Process (GP) to impute measurements along street canyons independent of the BS positions.

In this work, an environment-dependent approach is developed which incorporates real measured data and is independent of BS locations. All approaches from literature and our novel method REMIBRANDT are qualitatively compared in Tab. I.

III. PROPOSED HYBRID MACHINE LEARNING APPROACH REMIBRANDT

The objective of this work is to develop a hybrid ML model capable of reliable imputation of REMs with missing data values in the area of streets. This will be achieved by incorporating neighboring REM values, building information and cell information enriched by a sophisticated neighbour selection algorithm.

A. Data Preprocessing

Initially, RSRP measurements of each cell are rasterized into REMs for each cell. Grid points are removed artificially and used as labels for subsequent training and testing to emulate scenarios of incomplete data. Therefore, each point of the original REM is categorized as either a label or a neighbor feature with a certain probability preventing the ML model

TABLE I
COMPARISON OF LITERATURE APPROACHES FOR REM IMPUTATION.

Capabilities	Type	Analytical [4]	Ray Tracing [5]	DNN [6]	GP [7]	RF [8]	CNN [9]	RF REMIBRANDT
		Variable Resolution	X	X	X	-	X	X
Considers								
Building information		-	X	(X)	-	X	X	X
Measurements for calibration		-	-	X	X	X	X	X
Neighboring measurements		-	-	X	X	-	-	X
Independent of								
BS location		-	-	-	X	-	-	X
Measurement density		X	X	-	X	X	X	X

this work

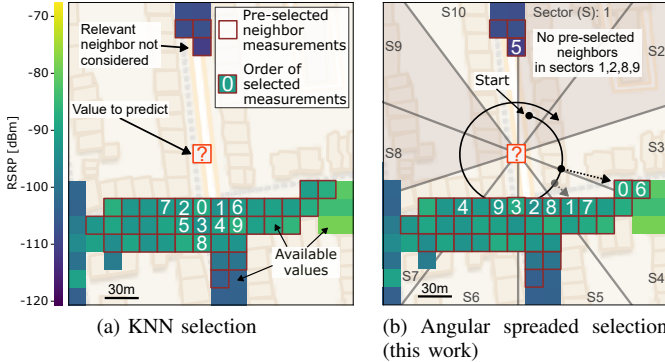


Fig. 3. Comparison of two approaches of selecting neighboring data. (Map data: © OpenStreetMap Contributors, CC BY-SA)

from learning dependencies of already seen labels. The optimal probability of assigning a point is determined by maximizing the number of labels while maintaining a minimum of nine neighbors in a $9\text{ m} \times 9\text{ m}$ area around the point to predict. Building footprints of the area are retrieved from OSM and rasterized in a $5 \times 5\text{ m}$ grid for faster processing.

B. Feature Engineering

The feature vector \mathbf{x} of REMIBRANDT is based on ten carefully selected neighbors and the corresponding feature set.

1) *Selection of neighboring points with angular spreading:* As illustrated in Fig. 3a, selecting the ten closest neighbors is not always the optimal choice, as it fails to consider relevant points in the northern region. Therefore, angular spreading determines ten neighbors out of 40 pre-selected closest neighbors. The pool of potential neighbors is limited to circumvent the processing of the entire REM, thereby reducing the processing time and focusing on nearby points. Each point is situated within one of the ten angular sectors illustrated in Fig. 3b. Beginning with *sector 1*, neighboring points are added circularly until a total number of ten points of neighboring RSRP features \mathbf{x}_{RSRP} is reached. In the situation of Fig. 3, angular spreading results in considering relevant points in the north, and the number of features for the ML is reduced.

2) *Position Features:* The distance and angle to selected neighboring features are used, to enable weighting of neighboring features appropriately. A sine and cosine encoding of the angle is added to the resulting positional feature vector \mathbf{x}_{pos} , in order to accommodate the cycling nature.

3) *Building Features:* As described in Sec. II, ML models can benefit from incorporating building features of the environment. Therefore, a radius around a neighboring point and a rectangle between the neighboring point and the point to be predicted are considered for the construction of building features as illustrated in Fig. 4. The *radius building features* \mathbf{x}_{rad_build} consider information about the mean and the standard deviation of the buildings within the radius r . *Rectangle building features* \mathbf{x}_{rect_build} additionally consider the number of buildings in the rectangular region of the width w and the offset o behind a point.

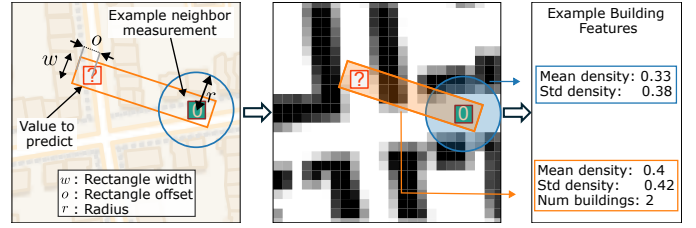


Fig. 4. Incorporating building information features into REMIBRANDT. (Map data: © OpenStreetMap Contributors, CC BY-SA)

4) *Cell Features:* Moreover, the general parameters of the cell (frequency and bandwidth), are considered as cell features \mathbf{x}_{cell} providing the ML model with static cell information.

C. Augmentation

Neighboring points have a high probability of being close to the point to be predicted. Therefore, an augmentation is performed to account for situations where neighboring points are situated at a greater distance. The process of angular spreading is conducted multiple times for minimum distances of 30 m, 60 m, 120 m and 240 m, respectively, in the pool of possible neighbors.

D. Machine Learning

The resulting feature vector for ten selected neighbors, $\mathbf{x} = [\mathbf{x}_{RSRP}, \mathbf{x}_{pos}, \mathbf{x}_{rad_build}, \mathbf{x}_{rect_build}, \mathbf{x}_{cell}]$, consists of 112 features in total. The effectiveness of different ML models is evaluated through a comparative analysis using the Root Mean Square Error (RMSE) metric on the test data set. A KNN, two tree-based approaches and a DNN are evaluated as ML approaches. The KNN operates on the closest neighboring measurements and take the mean of the ten selected neighboring RSRP values. The tree-based approaches are used because of their fast processing speed and favorable performance, as evidenced in [8]. Decision Trees (DTs) form the base entity of the two tree based approaches. RF [14] is an ensemble learning method that takes the average prediction of multiple DTs [15], which are trained using a random subset of variables. In contrast, the Extreme Gradient Boosting (XGBoost) [16] approach builds the DTs iteratively and weights the relevance of a learner in the context of the previously selected (fixed) base learner, using observation weights. Additionally, a DNN [17], based on layered neurons with a weighted connection to each neuron of the subsequent layer, is evaluated.

IV. METHODOLOGY OF THE TRAINING AND EVALUATION PROCESS

In order to evaluate the performance of the developed ML models, three different existing reference models are used:

- An ABG channel model,
- Empirical channel modeling with WINNER II, and
- the Okumura Hata channel model.

In contrast to the developed ML models, the BS positions area required for prediction. The predicted mean error of the three channel models to the given measurements is subtracted to account for the unknown constant parameters of the cell.

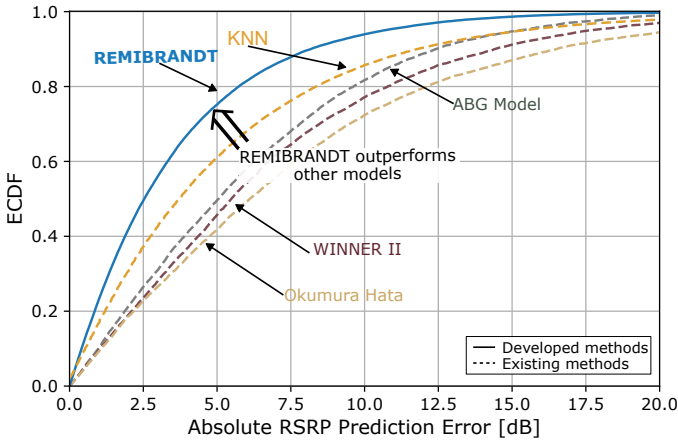


Fig. 5. An ECDF comparison of REMIBRANDT with existing analytical and empirical channel models.

The *Python* package *scikit-learn* [18] is used for model evaluation. Training and testing ML models on different data sets to evaluate the performance is crucial to prevent the model from overfitting by learning specific scenario-dependent features. Therefore, Dortmund is divided geographically into three data sets designated for training, validation during the hyperparameter process and testing to generalize the trained ML models. The distribution of measurements over each data set is 70%, 15% and 15%, respectively.

Determining the parameters that suit each ML model is vital to maximizing their performance. Therefore, hyperparameter tuning is performed for each ML model using a randomized grid search with 500 iterations and comparing the corresponding RMSE on the validation data set. The resulting hyperparameters of the RF used by REMIBRANDT are given in Tab. II, along with the tested hyperparameter distributions.

TABLE II
MODEL PARAMETERS DETERMINED FOR THE REMIBRANDT RF MODEL

Hyperparameters	Selected Value	Hyperparameter Grid
Min. samples split	12	[1, 2, 4, 6, ..., 12, 14, 16]
Max. depth	15	[10, 15, 20, ..., 140, 145, 150]
Min. samples leaf	2	[1, 2, 4, 6, 8]
Number of estimators	70	[10, 15, 20, ..., 140, 145, 150]

V. PERFORMANCE EVALUATION & TESTING ON REAL-WORLD SCENARIOS

The proposed REMIBRANDT model is evaluated alongside a KNN-based approach and empirical channel models on a held-out data set.

A. Machine Learning Model Selection

ML performance can be assessed by calculating single number metrics like the RMSE and by analyzing the error distribution. For this, the Empirical Cumulative Distribution Function (ECDF) of the different imputation methods is shown in Fig. 5. While the ABG channel model performs the best among the tested existing channel models, their performance lacks behind the KNN model and REMIBRANDT. The ABG

model also achieves a slightly higher RMSE of 7.88 dB compared to the 7.47 dB of the KNN model.

Different ML models have been tested for REMIBRANDT (RF, XGBoost, and DNN models). These perform about equally well, with a RMSE of 5.00 dB for the RF, 5.02 dB for XGBoost, and 5.01 dB for the DNN. Nevertheless, the RF model performs the best and is selected to be used with REMIBRANDT. REMIBRANDT exhibits a performance improvement of approximately 3 dB relative to the existing ABG channel model and 2.5 dB relative to the KNN approach.

Conventional channel models are analytical expressions that do not account for the nuances of actual scenarios. Similarly, empirical channel models are pre-fitted on a different scenario that may bear resemblance in the density of buildings but not in the actual structure of the scenario. These models cannot cope with the complexity of the scenario by considering the surrounding buildings and neighboring measurements in the same way REMIBRANDT does. Furthermore, expert knowledge is contributed by the sectorized feature generation approach (c.f. Sec. III), enabling REMIBRANDT to use it for imputation. If the angular spread approach-based feature selection is used for the KNN model a lower RMSE (6.30 dB) than the basic KNN model (7.47 dB) is achieved, too. However, REMIBRANDT is outperforming this approach too.

B. Artificially Removing Data in a Set Area for Imputation

Imputing larger areas of unknown channel quality is a challenging task of interest because some streets are not considered in the measurement process. Consequently, we compare the performance of REMIBRANDT with the KNN, a Ray Tracing (RT)-based approach, and the analytical ABG channel model on an example area with a dimension of approximately 500×500 m, as shown in Fig. 6. In order to simulate an automated tool chain, the RT-based approach utilizes the same building information as REMIBRANDT without any manual refinement. It assumes concrete buildings and the exact BS position. A radial antenna characteristic is assumed for the BS, and the gain is fitted on the known points.

All predictions reflect the general characteristic of decreasing signal strength over distance to the BS correctly. However, examining the absolute errors reveals that REMIBRANDT outperforms the other models. REMIBRANDT and the KNN model directly consider surrounding data, improving the transition from given measurements to the imputed previously removed area compared to the ABG model.

To accurately compare the error distribution in different regions of the test area, the absolute error of REMIBRANDT is subtracted from the absolute error of the other models. A yellow-tinted area indicates superior performance of REMIBRANDT, while a blue-tinted area indicates superior performance of the other model. When examining the difference between the KNN model and REMIBRANDT, it becomes evident that REMIBRANDT exhibits a lower absolute error in the majority of areas, except for a few isolated regions in the center. REMIBRANDT outperforms the ABG model by more than 15 dB in the majority of areas. The ABG model only

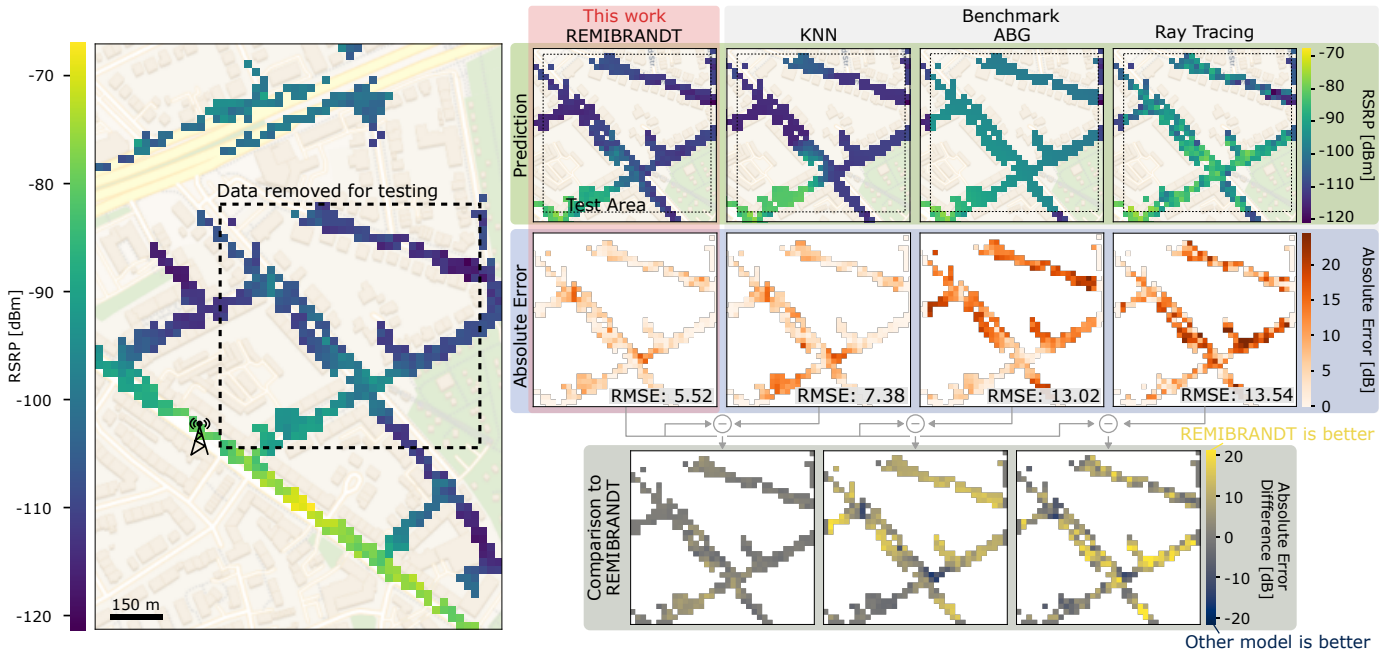


Fig. 6. Case study: Comparison of the imputation of the proposed REMIBRANDT approach with a KNN, a RT and an ABG channel model approach on removed ground truth points in rectangular test area. (Map data: © OpenStreetMap Contributors, CC BY-SA)

performs similarly in the southeastern region, which is close to the BS and has no shadowing. The RT approach displays better performance in a few isolated areas; however, in all other regions, REMIBRANDT demonstrates superior performance.

These findings illustrate that REMIBRANDT outperforms all other considered models in this scenario. This is particularly the case in complex situations that incorporate shadowing. In these situations, interpreting features correctly seems to be crucial and surrounding data from all directions needs to be considered.

C. Case Study: Using REMIBRANDT for ODD Dimensioning

In a case study, the impact of REM imputation for the accurate dimensioning of Operational Design Domains (ODDs) for teleoperation shall be analyzed based on one BS and REM cells of dimension 15×15 m. An ODD defines the area in which an application is known to be safely operated. By improving the accuracy, a smaller buffer zone for uncertainty needs to be incorporated and the ODD may be increased.

REMIBRANDT and a reference ABG channel model perform an imputation on 80% of the data, which are displayed underneath the original REM on the left side of Fig. 7. The remaining 20% are used for later validation. To determine the area where teleoperation is possible, the predicted signal strength is mapped into corresponding data rates using the formula given in [19]. The measured RSRP values are mapped to a corresponding Signal-to-Noise-Ratio (SNR) using

$$\text{SNR} = \text{RSRP} - 10 \cdot \log_{10}(k \cdot T \cdot \text{BW}_{\text{RSRP}}) - \text{NF}_{\text{UE}} - \text{NF}_{\text{BS}},$$

which was fitted on a cell in the area of the TU Dortmund University. Afterward, the data rate is calculated based on the parameters of the cell in the case study, as outlined in Tab. III. A comparison of the data rate with the minimum required data

rate allows for the categorization of each location as either a location where teleoperated driving is possible or a location where a cell change is necessary as illustrated on the left side of Fig. 7. Testing both models on the held-out data reveals that REMIBRANDT exhibits a 20% higher accuracy in predicting the feasibility of teleoperation within the examined cell. This accuracy becomes evident in the larger predicted ODD.

By subtracting the respective error of a 90% confidence level (c.f. Fig. 5) from the imputed RSRP, higher confidence in the prediction is reached, shown as a dark green area in Fig. 7. While this procedure reduces the overall accuracy, from 91.0% to 75.4% for REMIBRANDT, possible false positives are drastically decreased.

A serving area of the cell is defined, which corresponds to a potential area of responsibility of the cell for teleoperation. The results reveal that REMIBRANDT covers a larger area of the serving area of the cell while maintaining the same level of confidence. This is because more accurate predictions allow for lower security margins. Therefore, the deployment of REMIBRANDT for imputation can potentially reduce the number of BS required to ensure sufficient coverage for teleoperation.

VI. CONCLUSIONS

In this paper, we presented REMIBRANDT, a novel method for imputing REMs with missing measurement areas. REMIBRANDT is based on hybrid ML and does not require BS position data. Instead, it incorporates surrounding building information and neighboring measurements to impute the signal strength accurately. This approach enables REMIBRANDT to be used with arbitrary mobile network measurement data.

A comprehensive evaluation of a real-world dataset demonstrates that the proposed REMIBRANDT method is more

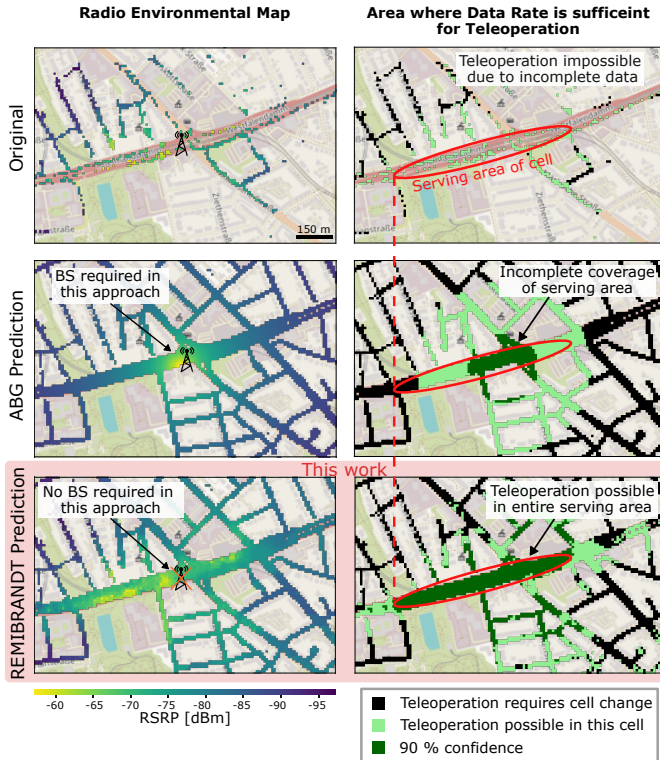


Fig. 7. The impact of the improved prediction performance of REMIBRANDT compared to the ABG approach on application ODD area planning based on a selected BS.

accurate than other methods despite not relying on BS locations. It achieves a 3 dB lower RMSE compared to the empirical ABG channel model. Thus, it allows for more precise planning for applications that rely on a set mobile network quality. In a teleoperation case study, the ODD predicted by REMIBRANDT matched the ground truth significantly better than the ABG model. Due to the higher prediction accuracy, the area of the predicted ODD of REMIBRANDT is larger than that of the ABG model for the same confidence level.

TABLE III
PARAMETERS OF THE CASE STUDY FOR ODD DIMENSIONING

Category	Parameter	Value
Cell Parameters	Technology	NR
	f	1800 MHz
	BW_{PRB}	30 MHz
	μ, ν_{layers}	1
	Overhead	0.08
	Q_m, R_{max}	MCS mapping of [20]
	$N_{PRB}^{BW, \mu}$	78 [21]
	T	300 K
	NF_{BS}, NF_{UE}	13 dB [22] 11 dB [22]
ODD Parameters	Minimum D	35 Mbit/s [2]
	Maximum speed	50 km/h

ML-based approaches rely on an extensive and well-generalizing training data set [23]. By further increasing the number of samples generated from sparse REMs, the prediction performance of REMIBRANDT over long distances may be improved in the future. In addition, further features could

be added to the feature vector to consider complex shadowing behavior even better, and unneeded features can be excluded.

ACKNOWLEDGMENT

This work has received funding by the German Federal Ministry of Education and Research (BMBF) in the course of the 6GEM research hub under grant number 16KISK038 and by the Federal Ministry of Transport and Digital Infrastructure (BMVI) in the context of the project *Virtual integration of decentralized charging infrastructure in cab stands* under the funding reference 16DKVM006B.

REFERENCES

- [1] A. Rostami, "Private 5G Networks for Vertical Industries: Deployment and Operation Models," in *Proc. IEEE 5GWF*, Nov. 2019.
- [2] 5GAA, "Tele-operated driving (ToD): System requirements analysis and architecture," 5GAA Automotive Association, Tech. Rep., Sep. 2021.
- [3] H. Schippers, S. Böcker, and C. Wietfeld, "Data-Driven Digital Mobile Network Twin Enabling Mission-Critical Vehicular Applications," in *Proc. IEEE 97th VTC-Spring*, Jun. 2023.
- [4] S. e. a. Sun, "Propagation Path Loss Models for 5G Urban Micro- and Macro-Cellular Scenarios," in *Proc. IEEE 83rd VTC-Spring*, May 2016.
- [5] Z. Yun and M. F. Iskander, "Ray Tracing for Radio Propagation Modeling: Principles and Applications," *IEEE Access*, Aug. 2015.
- [6] C. Han, H. Zhao, X. Liu, J. Yang, and C. Yuan, "Distributed Radio Map Modeling Based on Feature Augmentation of Augmented Scatter Graph," in *Proc. IEEE 34th PIMRC*, Sep. 2023.
- [7] L. Eller, P. Svoboda, and M. Rupp, "Propagation-Aware Gaussian Process Regression for Signal-Strength Interpolation along Street Canyons," in *Proc. IEEE 93rd VTC2021-Spring*, Apr. 2021.
- [8] M. Geis, B. Sliwa, C. Bektas, and C. Wietfeld, "TinyDRaGon: Lightweight Radio Channel Estimation for 6G Pervasive Intelligence," in *Proc. IEEE FNWF*, Oct. 2022.
- [9] L. Eller, P. Svoboda, and M. Rupp, "A Deep Learning Network Planner: Propagation Modeling Using Real-World Measurements and a 3D City Model," *IEEE Access*, vol. 10, pp. 122 182–122 196, Nov. 2022.
- [10] P. Kyösti *et al.*, "WINNER II channel models," IST, Report, Sep 2007.
- [11] T. Mahmood, H. K. AL-Qaysi, and A. S. Hameed, "The Effect of Antenna Height on the Performance of the Okumura/Hata Model Under Different Environments Propagation," in *Proc. IEEE CONIT*, 2021.
- [12] C. Ling, H. Chen, C. Li, Q. Qin, and X. Yin, "Characterization of mmWave and sub-6 GHz Propagation Channels in Manufacturing Scenarios," in *Proc. IEEE Globecom Workshops*, Dec. 2023.
- [13] A. Seretis and C. D. Sarris, "An Overview of Machine Learning Techniques for Radiowave Propagation Modeling," *IEEE Trans. on Antennas and Propagation*, vol. 70, no. 6, pp. 3970–3985, Jun. 2022.
- [14] L. Breiman, "Random Forests," *Machine Learning*, Oct. 2001.
- [15] L. Breiman, J. Friedman, R. A. Olshen, and C. J. Stone, *Classification and Regression Trees*. Chapman and Hall/CRC, Oct. 2017.
- [16] T. Chen and C. Guestrin, "XGBoost: A Scalable Tree Boosting System," in *Proc. 22nd ACM SIGKDD Int. Conf. on Knowl. Discovery and Data Mining*. ACM, Aug. 2016.
- [17] Y. LeCun, Y. Bengio, and G. Hinton, "Deep Learning," *Nature*, vol. 521, pp. 436–444, May 2015.
- [18] F. Pedregosa *et al.*, "Scikit-learn: Machine Learning in Python," *Journal of Machine Learning Research*, vol. 12, pp. 2825–2830, 2011.
- [19] 3GPP, "Study on self evaluation towards IMT-2020 submission," 3rd Generation Partnership Project (3GPP), Technical Report 37.910, Mar. 2024, version 18.0.0 Release 18.
- [20] L. Li, Q. Jiang, and W. Luo, "A Unified Non-CQI-based AMC Scheme for 5G NR Downlink and Uplink Transmissions," in *Proc. IEEE 6th ICCCS*, Apr. 2021.
- [21] 3GPP, "User Equipment (UE) radio transmission and reception; Part 1: Range 1 Standalone," 3rd Generation Partnership Project (3GPP), Technical Report 38.101, May 2022, version 17.5.0 Release 17.
- [22] 3GPP, "Study on International Mobile Telecommunications (IMT) parameters for 4400 - 4800 MHz, 7125 - 8400 MHz and 14800 - 15350 MHz," 3rd Generation Partnership Project (3GPP), Technical Specification (TS) 38.922, May 2024, version 0.1.0 Release 19.
- [23] P. Domingos, "A few useful things to know about machine learning," *Commun. ACM*, vol. 55, no. 10, p. 78–87, Oct. 2012.